Physics Letters B 753 (2016) 117–121

Contents lists available at ScienceDirect

Physics Letters B

www.elsevier.com/locate/physletb

ATLAS diboson excesses from the stealth doublet model

Wei Chao

Amherst Center for Fundamental Interactions, Department of Physics, University of Massachusetts-Amherst, Amherst, MA 01003, United States

ARTICLE INFO

Article history:
Received 21 July 2015
Received in revised form 1 December 2015
Accepted 1 December 2015
Available online 7 December 2015
Editor: J. Hisano

ABSTRACT

The ATLAS Collaboration has reported excesses in diboson invariant mass searches of new resonances around 2 TeV, which might be a prediction of new physics around that mass range. We interpret these results in the context of a modified stealth doublet model where the extra Higgs doublet has a Yukawa interaction with the first generation quarks, and show that the heavy CP-even Higgs boson can naturally explain the excesses in the WW and ZZ channels with a small Yukawa coupling, $\xi \sim 0.15$, and a tiny mixing angle with the SM Higgs boson, $\alpha \sim 0.05$. Furthermore, the model satisfies constraints from colliders and electroweak precision measurements.

1. Introduction

Excesses in searching for diboson resonance using boson-tagged jets were recently reported by the ATLAS Collaboration [1]. It shows local excesses in the WZ, WW and ZZ channels with significance of 3.4σ, 2.6σ and 2.9σ respectively. Similarly, the CMS Collaboration [2,3] has reported an excess of 1.9σ significance in the dijet resonance channel and $e\nu\bar{b}b$ channel which may arise from Wh with h decaying hadronically. These excesses may be evidences of new symmetries or new particles near 2 TeV.

Since the resonances decay into two gauge boson, they should be bosonic states. Possible origins of this excess were studied by several groups [4–23], where the excesses were explained as spin-1 gauge bosons [4,7,8,10–15,19] in an extended gauge group, composite spin-1 resonances [5,6,18], spin-0 or spin-2 composite particles [20–22] and extra scalar bosons [23,24]. The key points in explaining the excesses are the interactions of new resonance with the Standard Model (SM) gauge bosons, quarks and (or) gluons, the former of which is relevant to the branching ratio of the new resonance and the latter of which is relevant to the production of the new resonance at the LHC. One the one hand, one needs the couplings of new interactions to be large enough so as to give rise to a sizable production cross section at the LHC; on the other hand, the strengths of these interactions should be consistent with current constraints of colliders and electroweak precision measurements. These two requirements are mutual restraint. A new resonance is not able to explain the ATLAS excesses if its interaction strengths are not mutually compatible with these two requirements.

In this paper, we explain the ATLAS excesses in the stealth doublet model, where the second Higgs doublet, H_2, gets no vacuum expectation value, with mass near 2 TeV, and only the CP-even part of H_2 mixes with the SM Higgs boson. We assume H_2 has sizable Yukawa interaction with the first generation quarks, which is consistent with constraints of flavor physics. Such that the heavy CP-even Higgs boson can be produced at the LHC via the Yukawa interaction and can decay into diboson states through the mixing with the SM Higgs boson. Our numerical simulations show that one has $\sigma(pp \to H \to WW/ZZ) \sim 5$ fb by setting $\xi \sim 0.15$ and $\alpha \sim 0.05$, where ξ is the Yukawa coupling of the H_2 with the first generation quarks and α is the mixing angle between two CP-even neutral states. This result is consistent with current constraints from colliders and electroweak precision measurements.

The remaining of the paper is organized as follows: In section 2 we give a brief introduction to the model. Section 3 is the study of constraints on the model. We investigate the ATLAS diboson excesses arising from this stealth doublet model in section 4. The last part is the concluding remarks.

2. The model

We work in the modified stealth doublet model [25,26], where the second Higgs doublet gets no vacuum expectation value (VEV) but its CP-even part mixes with the SM Higgs boson. In the following, we first describe the modified stealth doublet model, and then study its implications in the ATLAS diboson excesses. The Higgs

E-mail address: chao@physics.umass.edu.

http://dx.doi.org/10.1016/j.physletb.2015.12.007

potential is the same as that in the general two Higgs doublet model (2HDM), which can be written as

$$V = -m_1^2 H_1^\dagger H_1 + m_2^2 H_2^\dagger H_2 + \left(m_{12}^2 H_1^\dagger H_2 + \text{h.c.}\right) + \lambda_1 (H_1^\dagger H_1)^2 + \lambda_2 (H_2^\dagger H_2)^2 + \lambda_3 (H_1^\dagger H_1)(H_2^\dagger H_2) + \lambda_4 (H_1^\dagger H_2)(H_2^\dagger H_1) + \left\{\frac{1}{2}\lambda_5 (H_1^\dagger H_2)^2 + (\lambda_6 H_1^\dagger H_1 + \lambda_7 H_2^\dagger H_2) H_1^\dagger H_2 + \text{h.c.}\right\} \quad (1)$$

In this paper, we assume the Higgs potential is CP-conserving, so all couplings in eq. (1) are real. Only one Higgs doublet gets nonzero VEV in the stealth doublet model, we take it be H_1. The tadpole conditions for the electroweak symmetry breaking become

$$m_1^2 = \lambda_1 v_1^2 , \qquad m_{12}^2 = -\frac{1}{2}\lambda_6 v_1^2 \quad (2)$$

where $v_1 = \sqrt{2}\langle H_1\rangle \approx 246$ GeV. After spontaneous breaking of the electroweak symmetry, there are two CP-even scalars h and H, one CP-odd scalar A and two charged scalars $C^\pm$, the mass eigenvalues of which can be written as [25]

$$m_A^2 = m_2^2 + \frac{1}{2}(\lambda_3 + \lambda_4 - \lambda_5) v_1^2 \quad (3)$$

$$m_C^2 = m_2^2 + \frac{1}{2}\lambda_3 v_1^2 \quad (4)$$

$$m_{h,H}^2 = \frac{1}{2}\left\{m_1^2 + m_A^2 + \lambda_5 v_1^2 \pm \sqrt{(m_1^2 - m_A^2 - \lambda_5 v_1^2)^2 - 4\lambda_6^2 v_1^4}\right\} \quad (5)$$

For convenience, we notate m_h as $\hat{m}_1$ and m_H as $\hat{m}_2$. The mixing angle α between h and H can be calculated directly, we take it as a new degree of freedom in this paper. H interacts with dibosons through the mixing. We refer the reader to Ref. [25] for the Feynman rules of Higgs interactions.

The Yukawa interactions of H_1 with SM fermions are exactly the same as the Yukawa interactions of the SM Higgs with fermions in the SM. We assume H_2 has sizable Yukawa coupling with the first generation quarks:

$$\mathcal{L}_N = \sqrt{2}\xi\, \overline{Q_1} \tilde{H}_2 u_R + \text{h.c.} \quad (6)$$

where $Q_1 = (u_L,\ d_L)^T$ and $\tilde{H}_2 = i\sigma_2 H_2^*$. Since $\langle H_2\rangle = 0$, there is almost no constraint on this Yukawa coupling, and H can be produced at the LHC via this interaction.

3. Constraints

Before proceeding to study ATLAS diboson excesses, let us investigate constraints on the mixing angle α. Couplings of the SM-like Higgs to other SM particles were measured by the ATLAS and CMS Collaborations. Comparing with SM Higgs couplings, couplings of h and H to all SM states (except u quark) are rescaled by $\cos\alpha$ and $\sin\alpha$, respectively:

$$g_{hXX} = \cos\alpha\, g_{hXX}^{\rm SM} , \qquad g_{HXX} = \sin\alpha\, g_{hXX}^{\rm SM} \quad (7)$$

where X represents SM states. Thus signal rates of the Higgs measurements relative to SM Higgs expectations are the functions of $\cos\alpha$. Performing a global χ^2 fit to the Higgs data given by ATLAS and CMS, one has $\cos\alpha \geq 0.84$ [27], at the 95% confidence level.

Another constraint comes from the oblique parameters [28,29], which are defined in terms of contributions to the vacuum polarizations of gauge bosons. The explicit expressions of ΔS and ΔT, which involve effects of all scalars, can be written as [30]

$$\Delta S = \frac{1}{\pi m_Z^2}\left\{ s^2 \sum_{i=1}^{2} (-1)^i [\mathcal{B}_2(m_Z^2; m_Z^2, \hat{m}_i^2) - m_Z^2 \mathcal{B}_0(m_Z^2; m_Z^2, \hat{m}_i^2)] + c^2 \mathcal{B}_2(m_Z^2; m_H^2, m_A^2) + s^2 \mathcal{B}_2(m_Z^2; m_h^2, m_A^2) - \mathcal{B}_2(m_Z^2; m_C^2, m_C^2)\right\} \quad (8)$$

$$\Delta T = \frac{1}{4\pi s_W^2 m_W^2}\{ s^2 B_2(0; m_C^2, m_h^2) + c^2 B_2(0; m_C^2, m_H^2) + B_2(0; m_C^2, m_A^2) - s^2 B_2(0; m_h^2, m_A^2) - c^2 B_2(0; m_H^2, m_A^2) - s^2 B_2(0; m_W^2, m_h^2) + s^2 B_2(0; m_W^2, m_H^2) + s^2 B_2(0; m_Z^2, m_h^2) - s^2 B_2(0; m_Z^2, m_H^2) + m_W^2 s^2 [B_0(0; m_W^2, m_h^2) - B_0(0; m_W^2, m_H^2)] + M_Z^2 s^2 [-B_0(0, m_W^2, m_h^2) + B_0(0; m_Z^2, m_H^2)] - \frac{1}{2} A_0(m_C^2)\} \quad (9)$$

where $\mathcal{B}_0(x; y, z) \equiv B_0(x; y, z) - B_0(0; y, z)$ and $\mathcal{B}_2(x; y, z) \equiv B_2(x; y, z) - B_2(0; y, z)$; the expressions of $B_0(x; y, z)$, $B_2(x; y, z)$ and $A_0(x)$ can be found in Ref. [30], $c = \cos\alpha$ and $s = \sin\alpha$, $s_W = \sin\theta_W$ with θ_W the weak mixing angle, M_Z and M_W are masses of Z and W bosons respectively.

The most recent electroweak fit (by setting $m_{h,ref} = 126$ GeV and $m_{t,ref} = 173$ GeV) to the oblique parameters performed by the Gfitter group [31] yields

$$S \equiv \Delta S^0 \pm \sigma_S = 0.03 \pm 0.10 , \qquad T \equiv \Delta T^0 \pm \sigma_T = 0.05 \pm 0.12 . \quad (10)$$

The $\Delta\chi^2$ can be written as

$$\Delta\chi^2 = \sum_{ij}^{2} (\Delta\mathcal{O}_i - \Delta\mathcal{O}_i^0)(\sigma^2)_{ij}^{-1}(\Delta\mathcal{O}_j - \Delta\mathcal{O}_j^0) \quad (11)$$

where $\mathcal{O}_1 = S$ and $\mathcal{O}_2 = T$; $\sigma_{ij}^2 = \sigma_i \rho_{ij} \sigma_j$ with $\rho_{11} = \rho_{22} = 1$ and $\rho_{12} = 0.891$.

As can be seen from eqs. (8) and (9), there are four free parameters contributing to the oblique parameters, m_A, m_C, m_H and α. To preform electroweak fit, we set $M_C = M_A \equiv M$, which can be easily achieved by setting $\lambda_3 = \lambda_4$, and $m_H = 2$ TeV, so that only two free parameters left. Blue points in the left panel of Fig. 1 show the contribution to the ΔS and ΔT by setting M and $\sin\alpha$ random parameters varying in the range $(1.8, 2.3)$ TeV and $(0, 1)$ respectively. The contour in the same plot shows the allowed region in the S–T plane in the 95% C.L. A direct numerical calculation shows that $|\sin\alpha| \leq 0.3$. In the right panel of Fig. 1 we show the region that is allowed by the oblique observations in the M_C–M_A plane by setting $\sin\alpha = 0.1$ and $M_H = 2$ TeV. To summarize, electroweak precision measurements put stronger constraint on the α even for the nearly degenerate heavy states.

The third constraint on this model is the perturbativity. Notice that the quartic coupling λ_6 is crucial for the mixing angle α, and the relationship between them can be written as $\sin 2\alpha = 2v^2\lambda_6/(m_H^2 - m_h^2)$. By requiring $m_H \sim 2$ TeV and $\lambda_6 < 4\pi$ (for a naive estimation of the perturbativity), one has $\alpha < 0.196$, which is the strongest constraint compared with these from Higgs measurements and oblique parameters.

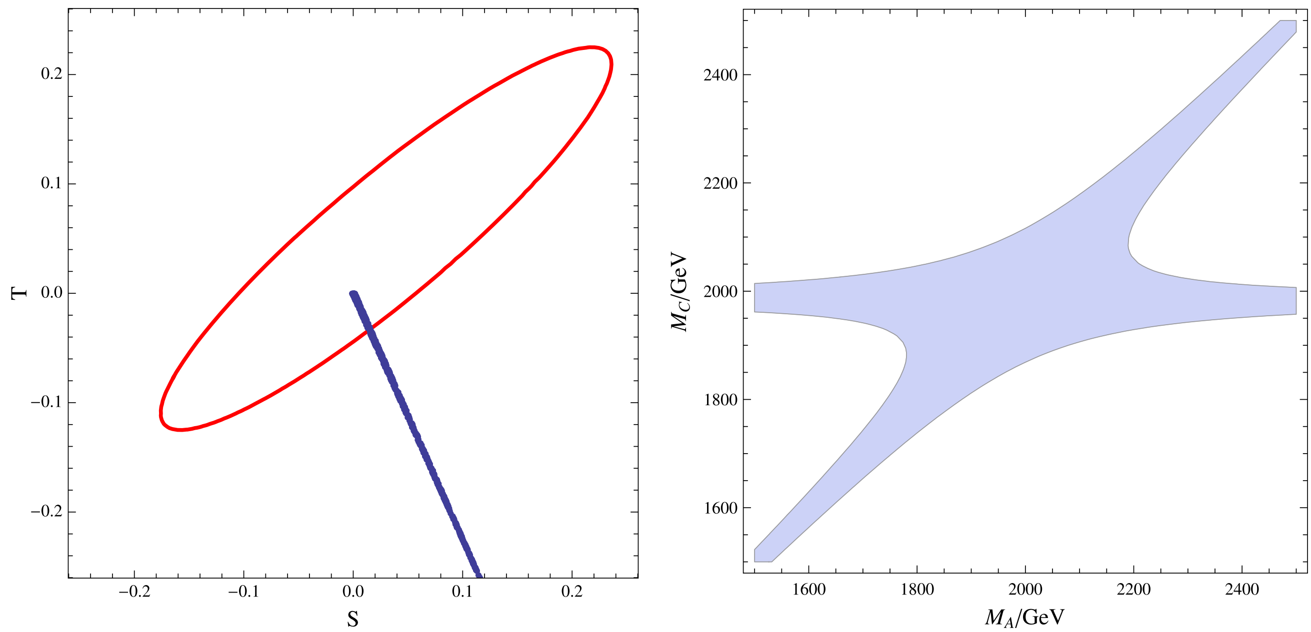

Fig. 1. Left panel: Predictions of heavy state in the S–T plane by setting $M_C = M_A$ and $M_H = 2$ TeV; Right panel: Constraints on the masses of the charged and CP-odd neutral states from oblique parameters by setting $m_H = 2$ TeV and $\sin\alpha \sim 0.1$. (For interpretation of the references to color in this figure legend, the reader is referred to the web version of this article.)

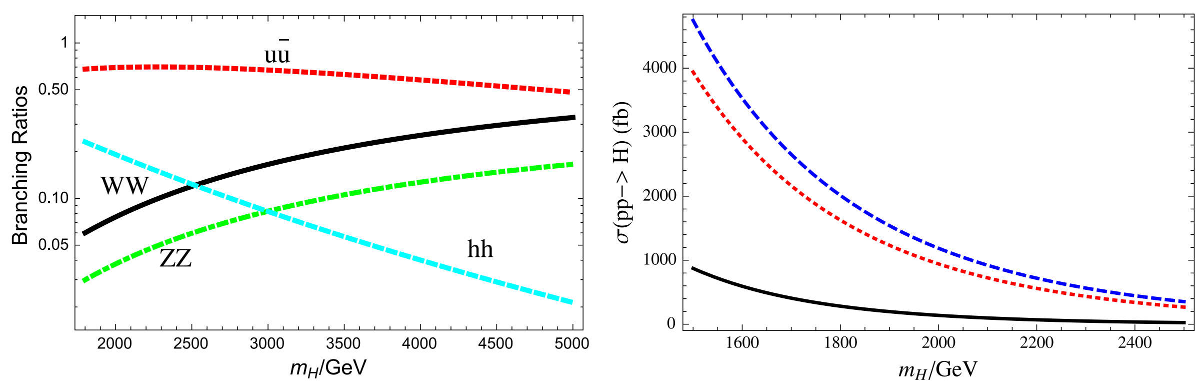

Fig. 2. Left panel: Branching ratios of H as the function of m_H by setting $s \sim 0.05$ and $\xi = 0.5$; Right panel: Production cross section of the heavy CP-even Higgs boson at the LHC by setting $\xi = 0.5$, with solid, dotted and dashed lines correspond to $\sqrt{s} = 8, 13, 14$ TeV respectively.

4. Diboson excesses

Heavy scalar states in our model can be produced at the LHC through its Yukawa interaction with the first generation quarks as was shown in eq. (6) and can decay into diboson final states from the mixing with the SM-like Higgs boson. The main decay channels of H are $\bar{u}u$, $\bar{t}t$, W^+W^-, ZZ and hh. The decay rates can be written as

$$\Gamma_{u\bar{u}} = \frac{c^2 n_C \xi^2 m_H}{8\pi} \tag{12}$$

$$\Gamma_{t\bar{t}} = \frac{s^2 n_C m_t^2 (m_H^2 - 4m_t^2)^{3/2}}{8\pi m_H^2 v^2} \tag{13}$$

$$\Gamma_{VV} = \frac{s^2 m_V^4 \sqrt{m_H^2 - 4m_V^2}}{4(1+\delta_V)\pi m_H^2 v^2}\left(3 - \frac{m_H^2}{m_V^2} + \frac{m_H^4}{4m_V^4}\right) \tag{14}$$

$$\Gamma_{hh} = \frac{c^4 v^2 \sqrt{m_H^2 - 4m_h^2}}{8\pi m_H^2}\left[(3\lambda_1 - \lambda_{345})s + \frac{3}{2}\lambda_6 c\right]^2 \tag{15}$$

where $n_C = 3$, being the color index; $V = W, Z$ respectively, $\delta_W = 0$, $\delta_Z = 1$ and $\lambda_{345} = \lambda_3 + \lambda_4 + \lambda_5$, which can be reconstructed by physical parameters. We show in the left panel of Fig. 2 the branching ratios of H by setting $s = 0.05$ and $\xi = 0.5$, where the solid, dot-dashed, dotted and dashed lines correspond to the branching ratios of WW/ZZ, $\bar{u}u$ and hh channels, respectively. We plot in the right panel of Fig. 2 the production cross section of H at the LHC, using the **CTEQ6.6** parton distribution functions (PDF) in [33]. The solid, dotted and dashed lines correspond to $\sqrt{s} = 8$ TeV, 13 TeV and 14 TeV, respectively.

We show in Fig. 3 the contours of $\sigma(pp \to H \to WW)$ in the $\sin\alpha$–ξ plane. The dashed, solid and dotted lines correspond to $\sigma(pp \to H \to WW) = 5, 10, 20$ fb respectively. The region marked by light-blue color is excluded by the oblique parameters. One can get similar numerical results for the $(pp \to H \to ZZ)$ process but with a larger ξ. The ATLAS reported number of excesses is about 8–9 events near the 2 TeV peak. Given a luminosity of 20.3 fb^{-1}, one has $\sigma(pp \to H \to WW) \approx 5$–6 fb for a 13% [1] selection efficiency of the event topology and boson-tagging requirements. Although large enough cross section can be produced at the LHC,

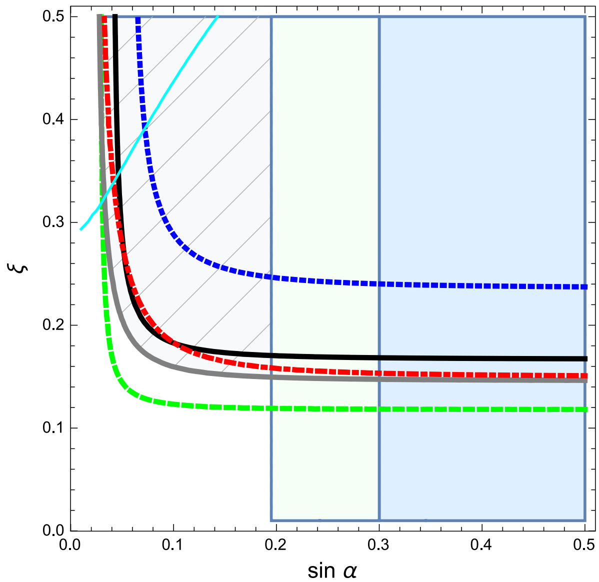

Fig. 3. Contour plot of $\sigma(pp \to H \to WW)$ in the $\sin\alpha$–ξ plane. The blue dotted, black solid and green dashed lines correspond to $\sigma(pp \to H \to WW) = 20, 10, 5$ fb respectively. The region below the gray solid line satisfies $\sigma(pp \to A \to hZ) < 7$ fb. The region below the red dot-dashed line satisfies $\sigma(pp \to C \to hW) < 7$ fb. The region below the cyan solid line has $\sigma(pp \to R \to jj) < 100$ fb. The region marked by light-blue color is excluded by the oblique parameters and the region marked by light-green color is excluded by the perturbativity. (For interpretation of the references to color in this figure legend, the reader is referred to the web version of this article.)

the model is constrained by other LHC experimental results. We will discuss these constraints one-by-one as follows:

- The CMS Collaboration [32] has reported an upper bound for the $\sigma(pp \to R \to W^+h)$, where R is a new resonance. It gives $\sigma(pp \to R \to W^+h) \le 7$ fb. The resonance can be the charged component of the heavy scalar doublet in our model. Its decay rate can be written as

$$\Gamma_{C\to Wh} = \frac{g^2 s^2}{64\pi m_W^2 m_C^3}\lambda^{3/2}(m_C^2, m_h^2, m_W^2)\,, \qquad (16)$$

  where $\lambda(x, y, z) = x^2 + y^2 + z^2 - 2xy - 2xz - 2yz$ and g is the $SU(2)$ gauge coupling. Fig. 3 shows the numerical results by setting $m_C = 2.2$ TeV, where the region below the red dot-dashed line satisfies this constraint.
- The CP-odd component of the heavy scalar doublet can be the mediator of the process $pp \to R \to Zh$, which was also measured by the CMS Collaboration. One has $\sigma(pp \to A \to Zh) < 7$ fb. The decay rate of $A \to Zh$ can be written as

$$\Gamma_{A\to Zh} = \frac{g^2 s^2}{64\pi c_W^2 m_Z^2 m_A^3}\lambda^{3/2}(m_A^2, m_Z^2, m_h^2) \qquad (17)$$

  where $c_W = \cos\theta_W$ with θ_W the weak mixing angle. A can also decay into dijet final states with the decay rate the same as that in eq. (12). We show in Fig. 3 the numerical results, where the region to the top-right of the gray solid line is excluded by this constraint.
- Both ATLAS and CMS have searched for resonances decaying into dijets. We use $\sigma(pp \to R \to jj) \le 100$ fb with the acceptance $\mathcal{A} \sim 0.6$. Both the CP-even and the CP-odd heavy scalars as well as the charged scalar in our model mainly decay into dijet via the Yukawa interaction. We show in Fig. 3 the region (to the bottom-right corner of the cyan solid line) allowed by this constraint.

Since the decay rate of $H \to t\bar{t}$ is tiny, there is almost no constraint on the model from $t\bar{t}$ resonance searches. As can be seen from Fig. 3, $\sigma(pp \to H \to WW)$ should be less than 6–7 fb. One has $\sigma(pp \to H \to WW) \sim 5$ fb for $\xi \sim 0.15$ and $\alpha \sim 0.05$, which is consistent with the constraints of colliders and electroweak precision measurements. No direct excess in the WZ channel comes out of our model. But the ATLAS observed excess in the WZ channel can be interpreted as the misidentification of the W/Z-tagged jet owing to uncertainties of the tagging selections.

Finally, we comment on two similar papers [23,24], which appeared while we were finalizing and submitting this paper. Both papers studied the possibilities of explaining the ATLAS diboson excesses in the framework of 2HDM. Our studies are similar but not the same. The difference is that we work in a special scenario where the Higgs eigenbasis equals to the scalar interaction eigenbasis. It is straightforward and clear to avoid problems arising from flavor physics in this scenario. Besides, couplings in the scalar sector can be easily reconstructed by physical parameters, we thus checked the influence of the heavy scalar to di-Higgs decay, which only slightly change the parameter space available for the ATLAS diboson excesses in this model.

5. Summary

We investigated the prospects of the stealth doublet model as a possible explanation to the diboson excesses observed by the ATLAS Collaboration. The mass of heavy Higgs boson was fixed at near 2 TeV in our study. We showed that excesses in the WW and ZZ channels can be interpreted as the decay of the heavy CP-even Higgs boson H, which can be produced at the LHC via its Yukawa interaction with the first generation quarks. One needs the Yukawa coupling $\xi \sim 0.15$ and the mixing angle between two CP-even Higgs bosons $\alpha \sim 0.05$, which is consistent with precision measurements, so as to have a 5 fb production cross section at the LHC. Constraints on the model from the exclusion limits in Wh and Zh channels given by CMS Collaboration and dijet searches were also studied, which showed the limited parameter space (in Fig. 3) that can be accommodated with the interpretation of the ATLAS diboson excesses in the same model. We expect the running of the 13 TeV LHC to tell us the detail about the diboson excesses and show us more clear hints of new physics behind this phenomena.

Acknowledgements

The author thanks to Huaike Guo and Peter Winslow for very helpful discussions. This work was supported in part by DOE Grant DE-SC0011095.

References

[1] G. Aad, et al., ATLAS Collaboration, arXiv:1506.00962 [hep-ex].
[2] V. Khachatryan, et al., CMS Collaboration, J. High Energy Phys. 1408 (2014) 173, arXiv:1405.1994 [hep-ex].
[3] V. Khachatryan, et al., CMS Collaboration, J. High Energy Phys. 1408 (2014) 174, arXiv:1405.3447 [hep-ex].
[4] J. Hisano, N. Nagata, Y. Omura, arXiv:1506.03931 [hep-ph].
[5] H.S. Fukano, M. Kurachi, S. Matsuzaki, K. Terashi, K. Yamawaki, arXiv:1506.03751 [hep-ph].
[6] D.B. Franzosi, M.T. Frandsen, F. Sannino, arXiv:1506.04392 [hep-ph].
[7] K. Cheung, W.Y. Keung, P.Y. Tseng, T.C. Yuan, arXiv:1506.06064 [hep-ph].
[8] B.A. Dobrescu, Z. Liu, arXiv:1506.06736 [hep-ph].
[9] J.A. Aguilar-Saavedra, arXiv:1506.06739 [hep-ph].
[10] Y. Gao, T. Ghosh, K. Sinha, J.H. Yu, arXiv:1506.07511 [hep-ph].
[11] A. Thamm, R. Torre, A. Wulzer, arXiv:1506.08688 [hep-ph].
[12] J. Brehmer, J. Hewett, J. Kopp, T. Rizzo, J. Tattersall, arXiv:1507.00013 [hep-ph].
[13] Q.H. Cao, B. Yan, D.M. Zhang, arXiv:1507.00268 [hep-ph].
[14] G. Cacciapaglia, M.T. Frandsen, arXiv:1507.00900 [hep-ph].

[15] T. Abe, R. Nagai, S. Okawa, M. Tanabashi, arXiv:1507.01185 [hep-ph].
[16] B.C. Allanach, B. Gripaios, D. Sutherland, arXiv:1507.01638 [hep-ph].
[17] T. Abe, T. Kitahara, M.M. Nojiri, arXiv:1507.01681 [hep-ph].
[18] A. Carmona, A. Delgado, M. Quiros, J. Santiago, arXiv:1507.01914 [hep-ph].
[19] B.A. Dobrescu, Z. Liu, arXiv:1507.01923 [hep-ph].
[20] C.W. Chiang, H. Fukuda, K. Harigaya, M. Ibe, T.T. Yanagida, arXiv:1507.02483 [hep-ph].
[21] G. Cacciapaglia, A. Deandrea, M. Hashimoto, arXiv:1507.03098 [hep-ph].
[22] V. Sanz, arXiv:1507.03553 [hep-ph].
[23] C.H. Chen, T. Nomura, arXiv:1507.04431 [hep-ph].
[24] Y. Omura, K. Tobe, K. Tsumura, Phys. Rev. D 92 (5) (2015) 055015, arXiv:1507.05028 [hep-ph].
[25] R. Enberg, J. Rathsman, G. Wouda, Phys. Rev. D 91 (9) (2015) 095002, arXiv:1311.4367 [hep-ph].
[26] R. Enberg, J. Rathsman, G. Wouda, J. High Energy Phys. 1308 (2013) 079, arXiv:1304.1714 [hep-ph];
R. Enberg, J. Rathsman, G. Wouda, J. High Energy Phys. 1501 (2015) 087 (Erratum).
[27] S. Profumo, M.J. Ramsey-Musolf, C.L. Wainwright, P. Winslow, Phys. Rev. D 91 (3) (2015) 035018, arXiv:1407.5342 [hep-ph].
[28] M.E. Peskin, T. Takeuchi, Phys. Rev. Lett. 65 (1990) 964.
[29] M.E. Peskin, T. Takeuchi, Phys. Rev. D 46 (1992) 381.
[30] H.E. Haber, D. O'Neil, Phys. Rev. D 83 (2011) 055017, arXiv:1011.6188 [hep-ph].
[31] M. Baak, M. Goebel, J. Haller, A. Hoecker, D. Kennedy, R. Kogler, K. Moenig, M. Schott, et al., Eur. Phys. J. C 72 (2012) 2205, arXiv:1209.2716 [hep-ph].
[32] V. Khachatryan, et al., CMS Collaboration, arXiv:1506.01443 [hep-ex].
[33] P.M. Nadolsky, H.L. Lai, Q.H. Cao, J. Huston, J. Pumplin, D. Stump, W.K. Tung, C.-P. Yuan, Phys. Rev. D 78 (2008) 013004, arXiv:0802.0007 [hep-ph].